Talanta 97 (2012) 331–335

Contents lists available at SciVerse ScienceDirect

Talanta

journal homepage: www.elsevier.com/locate/talanta

Colorimetric detection of Mn^{2+} using silver nanoparticles cofunctionalized with 4-mercaptobenzoic acid and melamine as a probe

Ying Zhou [a], Hong Zhao [a,*], Chang Li [a], Peng He [a], Wenbo Peng [a], Longfei Yuan [a], Lixi Zeng [a], Yujian He [a,b,**]

[a] College of Chemistry and Chemical Engineering, Graduate University of Chinese Academy of Sciences, 19A YuQuan Road, Beijing 100049, China
[b] State Key Laboratory of Natural and Biomimetic Drugs, Peking University, Beijing 100191, China

ARTICLE INFO

Article history:
Received 19 December 2011
Received in revised form
10 April 2012
Accepted 21 April 2012
Available online 11 May 2012

Keywords:
Colorimetric detection
Silver nanoparticles
4-Mercaptobenzoic acid
Melamine
Mn^{2+}

ABSTRACT

A facile, selective and highly sensitive method is proposed for colorimetric detection of manganese ions using 4-mercaptobenzoic acid (4-MBA) and melamine (MA) modified silver nanoparticles (AgNPs). The presence of Mn^{2+} induces the aggregation of AgNPs through cooperative metal–ligand interaction, resulting in a color change from bright yellow to purple. The cofunctionalized AgNPs showed obvious advantages over the ones functionalized only by 4-MBA or MA in terms of selectivity. Mn^{2+} could be monitored by colorimetric response of AgNPs by a UV–vis spectrophotometer or even naked eyes. The absorbance ratio ($A_{550\ nm}/A_{408\ nm}$) is linear with the concentration of Mn^{2+} ranging from 5×10^{-7} mol/L to 1×10^{-5} mol/L with a correlation coefficient of 0.993, and the detection limit is as low as 5×10^{-8} mol/L. Particularly, this cost-effective process also allowed rapid and simple determination of the Mn^{2+} in drinking water.

1. Introduction

Some metal ions are crucial components of living organisms, serving as cofactors for numerous proteins with diverse functions [1]. Mn^{2+} is one of essential trace elements, and it is an important component of several endogenous antioxidant enzymes, such as catalase and superoxide dismutases [2]. It is significant for the metabolism of our body and various biological processes below certain amounts. However, uptake of high concentration of Mn^{2+} is harmful and causes central nervous system disorders, such as Parkinson's disease and so on [3]. Therefore it is necessary to develop methods for detecting it at low concentrations in samples with great precision and accuracy.

In recent years, various methods for the determination of manganese have been reported, including electron spectroscopy [4]. Diphenylphosphine (DPP) [5], chemical modifer-Electrothermal Atomic Absorption Spectrometry (ETAAS) [6], and crosslinked chitosan-Flame Atomic Absorption Spectrometry (FAAS) [7]. More recently, Goodwin and co-workers have proposed a method for the detection of manganese in seawater by a cathodic stripping voltammetry using a boron-doped diamond electrode [8]. Robaina reported a sensor for the direct determination of manganese in waters extracted during petroleum exploitation by Electrothermal Atomic Absorption Spectrometry (ET AAS) using Ir–W as permanent modifier [9]. Jaime and co-workers proposed a spectrophotometric method to quantify dissolved manganese in marine pore waters, using Cadmium (II) meso-Tetrakis (4-sulfophenyl) porphyrin (Cd-TSPP) complex as an indicator [10]. However, most of these techniques need costly instruments or complex procedures, making them inconvenient and time-consuming [11].

Colorimetric sensors have attracted increasing consideration for their convenience of visual observation and simple operations in recent years [12–17]. Compared with other assays, they allow direct and on-site analysis of the samples with the naked eye. Among colorimetric sensors, Ag nanoparticles-based colorimetric sensors have many advantages over gold nanoparticles-based ones, such as higher extinction coefficients and lower prices, allowing detection with minimal material consumption [18]. Thus, glutathione-stabilized silver nanoparticles have been used to determine Ni^{2+} [19]. Bifunctionalized triazole-carboxyl AgNPs have been used to recognize Co^{2+} in aqueous solution [20]. However, the challenge to produce a colorimetric sensor for metallic ions detections is to find a suitable mediator to modify the surface of silver nanoparticles, which links AgNPs together through metal–ligand interaction.

In this paper, Ag nanoparticles modified with 4-mercaptobenzoic acid and melamine were used as selective colorimetric sensors for

* Corresponding author. Fax: +86 010 88256141.
** Corresponding author at: College of Chemistry and Chemical Engineering, Graduate University of Chinese Academy of Sciences, 19A YuQuan Road, Beijing 100049, China. Fax: +86 010 88256141.
E-mail addresses: hongzhao@gucas.ac.cn (H. Zhao), heyujian@gucas.ac.cn (Y. He).

0039-9140/$ - see front matter © 2012 Elsevier B.V. All rights reserved.
http://dx.doi.org/10.1016/j.talanta.2012.04.041

Mn^{2+}. As far as we know, –SH of 4-Mercaptobenzoic acid and $–NH_2$ of melamine can both interact with AgNPs. As a result, the group –COOH of 4-Mercaptobenzoic acid and $–NH_2$ of melamine were modified on the surface of Ag nanoparticles together. It has been reported that both of the two groups have strong affinity to metal ions [21,22]. Based on this fact, AgNPs capped with 4-MBA and melamine aggregated in the presence of Mn^{2+} because of the ion-templated chelation. The cofunctionalized silver nanoparticles with –COOH and $–NH_2$ can have a cooperative effect on the recognition of Mn^{2+}, resulting in appreciable changes in color by naked eyes and absorption properties over other metal ions tested. To the best of our knowledge, this is the first report of Mn^{2+} colorimetric sensor using Ag nanoparticles. To demonstrate the practicality of the present approach, it has been successfully applied to determine the concentration of Mn^{2+} in drinking water.

2. Experimental

2.1. Chemicals and materials

All reagents were of analytical grade and used without further purification. Solutions were prepared using high pure water with a resistance of 18 MΩ.cm. 4-MBA was bought from Tokyo Chemical Industry Co., Ltd (Japan). Melamine was purchased from Sigma (USA). $AgNO_3$, $NaBH_4$, $MnSO_4$ and other metal ions were purchased from Beijing Chemical Company (Beijing, China). UV–vis absorption spectra were acquired on a UV-2550 spectrophotometer (Shimadzu, Japan), using 1-cm path length quartz cuvettes for measurements. IR spectra were measured with FT-IR spectrometer (Avatar 360, ESP). Transmission electron microscopy (TEM) measurements were made on an H-7500 (Hitachi, Japan) at 80 kV. The pH of the solution was measured with PB-10 pH meter (Sartorius, 91 Germany).

2.2. Probe preparation

AgNPs were prepared by the reduction of $AgNO_3$ with $NaBH_4$. Under vigorously magnetic stirring, 0.010 g $NaBH_4$ was added rapidly into 100 mL aqueous solution of $AgNO_3$ with final concentration of 1×10^{-4} mol/L, producing a light yellow colored solution. After stirring for 10 min, AgNPs solution was prepared.

To obtain 4-MBA-MA-AgNPs, 2 mL of 1×10^{-4} mol/L 4-MBA and 4 mL of 1×10^{-4} mol/L MA were both added to the prepared AgNPs and left to stir for about 0.5 h to make sure self-assembly of the 4-MBA and MA onto the surface of silver nanoparticles. 4-MBA-AgNPs were obtained by adding 2 mL 1×10^{-4} mol/L 4-MBA aqueous solution into the AgNPs with stirring for 0.5 h. MA-AgNPs were obtained by the same method. All of the experiments were prepared at room temperature.

3. Results and discussion

3.1. Characterization

To investigate the modification of 4-MBA-MA-AgNPs, FT-IR spectroscopy was performed. From Fig. 1, the characteristic absorption peak of –SH at 2559 cm^{-1} in pure 4-MBA had disappeared in the FT-IR spectra of 4-MBA-MA-AgNPs, indicating that 4-MBA had been successfully modified onto the surface of silver nanoparticles via the –SH group of 4-MBA. Comparing with MA, the 3000–3500 cm^{-1} peaks correspond to –NH vibrations, and these vibrations were shifted in the FT-IR spectra of 4-MBA-MA-AgNPs, revealing that MA interacted with AgNPs through $–NH_2$ group. The spectroscopy also showed that the –COOH group of 4-MBA at 1681 cm^{-1} appeared in 4-MBA-MA-AgNPs. From all of the above results, it can be concluded that –SH group and $–NH_2$ group are responsible for the formation of the cofunctionalized 4-MBA-MA-AgNPs. The FT-IR results further prove the fact that the function groups of –COOH and $–NH_2$ have been successfully attached onto the surface of AgNPs.

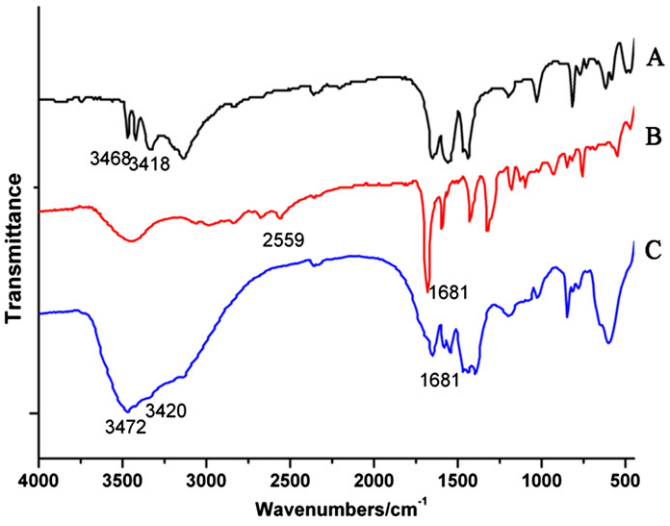

Fig. 1. FT-IR spectra of (A) MA, (B) 4-MBA and (C) 4-MBA-MA-AgNPs.

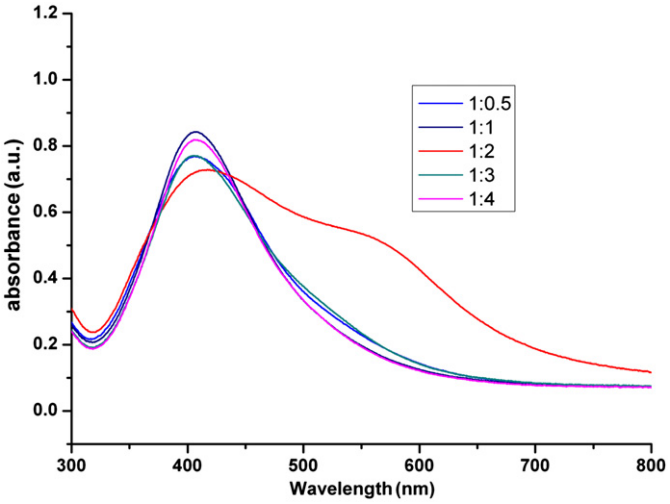

Fig. 2. The UV–vis spectra of 4-MBA-MA–AgNPs solutions modified with different ratio of 4-MBA and MA when adding 1×10^{-5} mol/L Mn^{2+} solution.

3.2. Effect of the ratio of the two modifiers

To investigate the effect of the ratio of the two modifiers (MA and 4-MBA) on the selectivity and sensitivity of the probe, the two modifiers were added to the AgNPs solutions in different proportion. Then Mn^{2+} solution was added, making the concentration of Mn^{2+} be 1×10^{-5} mol/L. As shown in Fig. 2, when the ratio of 4-MBA and MA was 1:2 (2 mL of 1×10^{-4} mol/L 4-MBA and 4 mL of 1×10^{-4} mol/L MA), Ag nanoparticles show obvious UV–vis spectroscopy absorption change since the absorbance ratio ($A_{550\ nm}/A_{408\ nm}$) increased apparently, while obvious change in the UV–vis spectroscopy absorption could not be observed when the ratio of 4-MBA and MA was 1:0.5, 1:1, 1:3 or 1:4. Based on these results, the ratio of the two modifiers (MA and 4-MBA) was chosen to be 1:2 in the following experiments.

3.3. Effect of pH

The pH condition for colorimetric detection of Mn^{2+} was optimized over the range from 7.0 to 11.0. When the pH value was less than 7.0, 4-MBA-MA-AgNPs were unstable and aggregated easily, which could be attributed to the formation of intermolecular hydrogen bonding between 4-MBA and MA in acidic solution. As shown in Fig. 3, when 1×10^{-5} mol/L Mn^{2+} solution was added, Ag nanoparticles show obvious UV–vis spectroscopy absorption change at pH=8, as Mn^{2+} induces the aggregation of Ag nanoparticles. However, at the neutral pH, the absorption showed little change. 4-MBA-MA-AgNPs were also nearly dispersed at pH=9, 10 and 11, this phenomenon showed Mn^{2+}-induced aggregation of the cofunctionalized Ag nanoparticles is blocked at the high pH value. Therefore, pH=8 was selected for further experiments considering the preferable sensitivity.

3.4. Colorimetric detection of Mn^{2+}

To further demonstrate the assay for the direct colorimetric visualization of Mn^{2+}, different amounts of Mn^{2+} were added to aqueous suspensions of 4-MBA-MA–AgNPs and tested after mixed for about 5 min. Fig. 4A reveals that the presence of Mn^{2+} led to red-shift of the peak at 408 nm and a new peak appeared at about 550 nm by UV–vis spectroscopy. The increase of Mn^{2+} concentration would induce a decrease of AgNPs' maximal absorption at 408 nm accompanying an obvious enhancement of the new peak at 550 nm, which indicated that the aggregating of AgNPs has a relationship with the concentration of Mn^{2+}. Under the optimum conditions, the colorimetric assay was processed using AgNPs to detect a series of Mn^{2+} with different concentrations ranging from 1×10^{-6} mol/L to 1×10^{-5} mol/L, a clear color progression from yellow to orange to purple with increasing Mn^{2+} concentration was observed (Fig. 4B). In other words, we can probably discriminate the concentration of Mn^{2+} with the naked eye compared with the stand colorimetric picture. A direct evidence for Mn^{2+}-stimulated aggregation of the AgNPs could be further supported by transmission electron microscopy (TEM) measurements. Fig. 5 showed the TEM images of AgNPs in the absence and presence of 1×10^{-5} mol/L Mn^{2+}. In the absence of Mn^{2+}, AgNPs were well dispersed in aqueous solution (Fig. 5A). On the other hand, irreversible aggregation occurs when added in Mn^{2+} (Fig. 5B). These results clearly indicate that the addition of trace Mn^{2+} could readily lead to the aggregation of AgNPs.

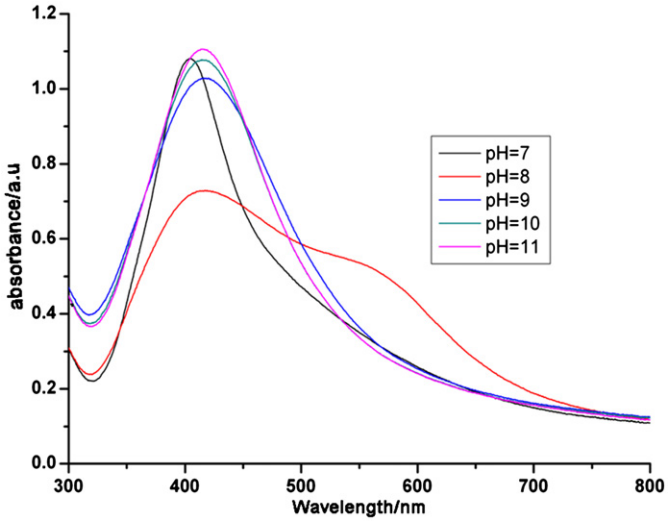

Fig. 3. The UV–vis spectra of 4-MBA-MA–AgNPs solutions with different pH ranging from 7.0 to 11.0 when adding 1×10^{-5} mol/L Mn^{2+} solution.

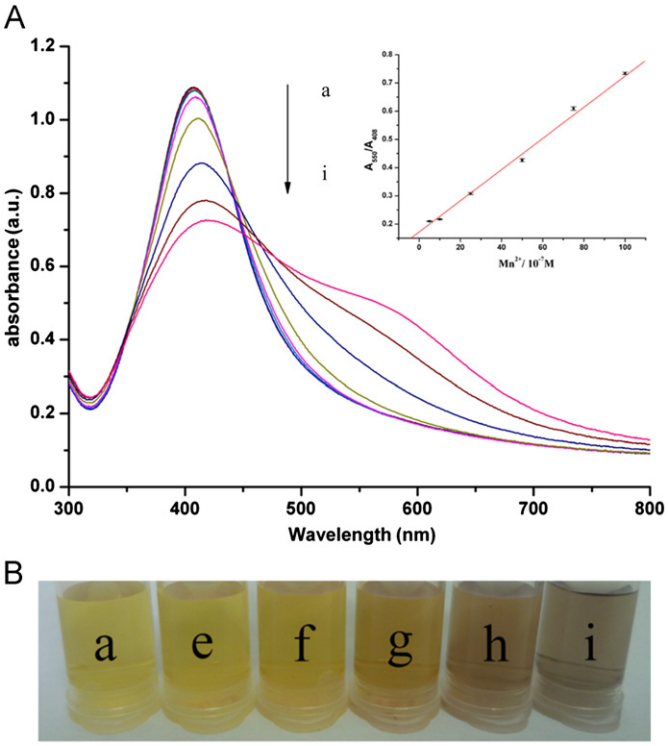

Fig. 4. (A) The UV–vis spectra of 4-MBA-MA–AgNPs solutions with various concentrations of Mn^{2+} ranging from 5×10^{-8} mol/L to 1×10^{-5} mol/L. (From a to i, the concentrations of Mn^{2+} are a: 0, b: 5×10^{-8}, c: 1×10^{-7}, d: 5×10^{-7}, e: 1×10^{-6}, f: 2.5×10^{-6}, g: 5×10^{-6}, h: 7.5×10^{-6}, i: 1×10^{-5} mol/L.) and plot of the absorbance $A_{550\ nm}/A_{408\ nm}$ of the AgNPs versus the Mn^{2+} concentrations: 5×10^{-7}, 1×10^{-6}, 2.5×10^{-6}, 5×10^{-6}, 7.5×10^{-6}, 1×10^{-5} mol/L. (B) Photographs of a solution of 4-MBA-MA–AgNPs in the absence (a) or presence of Mn^{2+} (e-i).

Quantitative analysis was performed by adding different concentrations of Mn^{2+} into AgNPs and monitoring the max absorption by UV–vis spectra. We obtained a linear correlation existed between the absorbance ratio ($A_{550\ nm}/A_{408\ nm}$) and Mn^{2+} concentration ranging from 5×10^{-7} mol/L to 1×10^{-5} mol/L with a correlation coefficient of 0.993 (inset to Fig. 4A). The detection limit for Mn^{2+} ions was approximately 5×10^{-8} mol/L (S/N=3). Although the detection limit is not as low as those obtained by some other methods [9], our assay has distinctive advantages such as simplicity, rapidness and low cost.

3.5. Selectivity of 4-MBA-MA-AgNPs

To investigate the selectivity of 4-MBA-MA-AgNPs, metal ions of the same concentration with 1×10^{-5} mol/L were added into the solution of AgNPs. As shown in Fig. 6B, in the presence of Mn^{2+}, a dramatic increase in the absorbance ratio ($A_{550\ nm}/A_{408\ nm}$) was clearly observed, whereas no obvious change was obtained in the presence of other metal ions. In Fig. 6A, c displayed the photographic images of 4-MBA-MA-AgNPs solution after adding various metal ions for 5 min, only the presence of Mn^{2+} ion induces a distinct color change from yellow to deep purple. The results demonstrated that this sensing system is specific to Mn^{2+} ions.

To further demonstrate the assay for the selected colorimetric visualization of Mn^{2+}, we had employed MA-AgNPs and

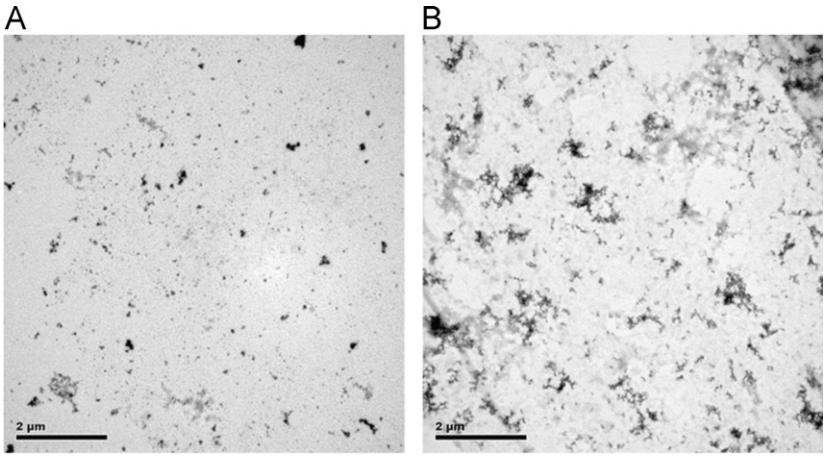

Fig. 5. TEM images of the 4-MBA-MA-AgNPs formed in the absence (A) and presence of (B) 1.0×10^{-5} mol/L Mn^{2+}.

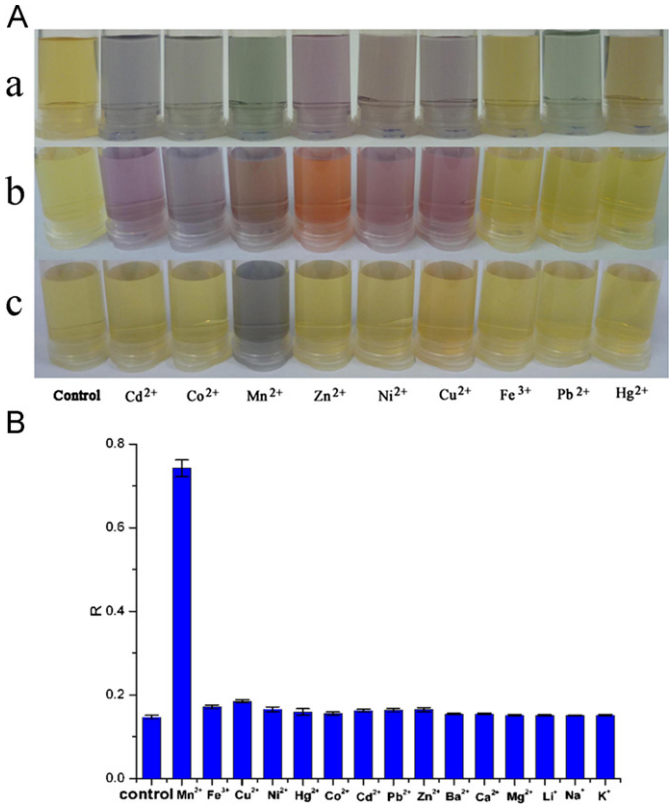

Fig. 6. A: Photographic images of (a) MA-AgNPs, (b) 4-MBA-AgNPs, and (c) 4-MBA-MA-AgNPs solution in the presence of 1×10^{-5} mol/L different metal ions. B: UV–vis spectra of 4-MBA-MA–AgNPs in the presence of 1×10^{-5} mol/L Mn^{2+} or other interferences.

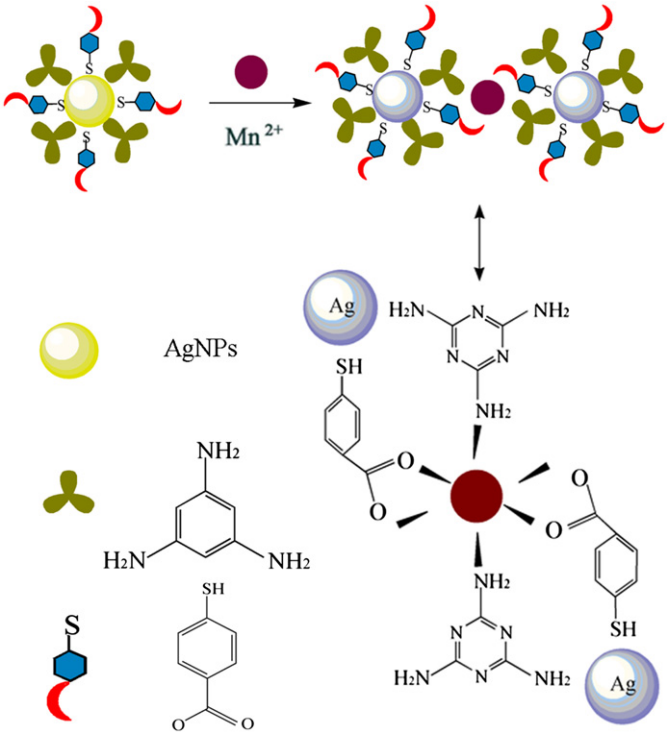

Fig. 7. Schematic of Mn^{2+} induced 4-MBA-MA-AgNPs aggregation.

4-MBA -AgNPs NPs as a control. From Fig. 6A, we can see the presence of most metal ions resulted in obvious color change of MA-AgNPs (Fig. 6A a) and 4-MBA–AgNPs (Fig. 6A b). However, only the presence of Mn^{2+} resulted in the color change of 4-MBA-MA-AgNPs, demonstrating that cofunctionalized AgNPs decorated with carboxyl and amino groups exhibited an excellent selectivity for the recognition of Mn^{2+}. The possible mechanism may be carboxyl and amino groups have a cooperative effect to form ion-templated chelation with Mn^{2+}. As shown in Fig. 7, the carboxyl group in the 4-MBA and amino in the MA can form a six-coordinated structure with manganese, which is similar with the reported literatures [23–25]. Therefore, the cofunctionalized AgNPs showed an excellent recognition of Mn^{2+}.

3.6. Drinking water sample analysis

To validate the applicability of our proposed sensing strategy for the analysis of real samples, standard addition method was used to detect drinking water according to most relative publications [20,26,27]. A series of Mn^{2+} standard solution was added into the drinking water, and then detected utilizing 4-MBA-MA-AgNPs based colorimetric method and Flame Atomic Absorption Spectrometry, respectively. The results were shown in Table 1, the recovery obtained by colorimetric method was in good agreement with these obtained by FAAS. Therefore, 4-MBA-MA-AgNPs probe is a practical tool for the determination of Mn^{2+} in drinking water samples.

Table 1
Comparison of recovery between flame atomic absorption spectrometry and the proposed colorimetric method for the detection of Mn^{2+} in drinking water.

	Sample	Added (μmol/L)	Found(μmol/L) mean ± SD	Recovery (%)
FAAS	1	6	5.86 ± 0.0037	97.7
	2	8	7.85 ± 0.0016	98.1
	3	10	10.18 ± 0.0021	101.8
Colori-	1	6	5.76 ± 0.0020	96.0
metric	2	8	8.25 ± 0.0018	103.1
Method	3	10	10.27 ± 0.0009	102.7

4. Conclusions

In summary, a colorimetric sensor for the detection of manganese ions using 4-MBA-MA modified silver nanoparticles (AgNPs) was proposed. The presence of Mn^{2+} induced the aggregation of AgNPs through cooperative metal–ligand interaction, resulting in a color change from bright yellow to purple. The cofunctionalized AgNPs showed obvious advantages over the ones functionalized only by 4-MBA or MA in terms of selectivity. Mn^{2+} could be monitored by colorimetric response of AgNPs by a UV–vis spectrophotometer or even naked eyes. The absorbance ratio ($A_{550\ nm}/A_{408\ nm}$) is linear with the concentration of Mn^{2+} ranging from 5×10^{-7} mol/L to 1×10^{-5} mol/L with a coefficient of 0.993, and the detection limit is as low as 5×10^{-8} mol/L. Particularly, the proposed method could be successfully applied to determine Mn^{2+} in drinking water. Therefore, this efficient and convenient colorimetric detection of Mn^{2+} at ambient temperature allows colorimetric sensors to be developed for widespread use.

Acknowledgment

This work was sponsored by the Major national scientific research plan (2011CB933202), the National Natural Science Foundation of China (Grant nos. 20877099 and 20972183), National Sci-Tech Major Special Item for Water Pollution Control and Management (Grant no. 2009ZX07527-007-03), National Key Technology Support Program (Grant no. 2009BAK61B01), the State Key Laboratory of Environmental Chemistry and Ecotoxicology (no. KF2010-23), the State Key Laboratory of Natural and Biomimetic Drugs (Grant no. K20120201) and the State Key Laboratory of Electroanalytical Chemistry (Grant no. SKLEAC2010005).

References

[1] R.H. Holm, P. Kennepohl, E.I. Solomon, Chem. Rev. 96 (1996) 2239.
[2] J.R. Wispe, B.B. Warner, J.C. Clark, C.R. Dey, J. Neuman, S.W. Glasser, J.D. Crapo, L.Y. Chang, J.A. Whitsett, J. Biol. Inorg. Chem. 267 (1992) 23937.
[3] G. Oszlanczi, T. Vezer, L. Sarkozi, E. Horvath, Z. Konya, A. Papp, Ecotox. Environ.Safe 73 (2010) 2004.
[4] M. Zaw, B. Chiswell, Talanta 42 (1995) 27.
[5] G.W. Luther, D.B. Nuzzio, J. Wu, Anal. Chim. Acta 284 (1994) 473.
[6] C.R. Lan, Z.B. Alfassi, Analyst 119 (1994) 1033.
[7] K. Kargosha, M. Noroozifar, Anal. Chim. Acta 413 (2000) 57.
[8] A. Goodwin, A.L. Lawrence, C.E. Banks, F. Wantz, D. Omanovic, E. Komorsky-Lovric, R.G. Compton, Anal. Chim. Acta 533 (2005) 141.
[9] R.J. Cassella, L.G.T. dos Reis, R.E. Santelli, E.P. Oliveira, Talanta 85 (2011) 415.
[10] J. Soto-Neira, Q.Z. Zhu, R.C. Aller, Mar. Chem. 127 (2011) 56.
[11] P.J. Chapman, Z. Long, P.G. Datskos, R. Archibald, M.J. Sepaniak, Anal. Chem. 79 (2007) 7062.
[12] R. Elghanian, J.J. Storhoff, R.C. Mucic, R.L. Letsinger, C.A. Mirkin, Science 277 (1997) 1078.
[13] J.J. Storhoff, R. Elghanian, R.C. Mucic, C.A. Mirkin, R.L. Letsinger, J. Am. Chem. Soc. 120 (1998) 1959.
[14] F. Li, Y. Feng, C. Zhao, B. Tang, Biosens. Bioelectron. 26 (2011) 4628.
[15] Y.C. Cao, R.C. Jin, S. Thaxton, C.A. Mirkin, Talanta 67 (2005) 449.
[16] H.X. Li, L. Rothberg, Proc. Natl. Acad. Sci. USA 101 (2004) 14036.
[17] F. Li, Y. Feng, C. Zhao, P. Li, B. Tang, Chem. Commun. 48 (2012) 127.
[18] J.S. Lee, A.K.R.L. Jean, S.J. Hurst, C.A. Mirkin, Nano Lett. 7 (2007) 2112.
[19] H.B. Li, Z.M. Cui, C.P. Han, Sens. Actuators B 143 (2009) 87.
[20] Y. Yao, D.M. Tian, H.B. Li, ACS Appl. Mater. Inter. 2 (2010) 684.
[21] J. Aguado, J.M. Arsuaga, A. Arencibia, M. Lindo, V.J. Gascon, Hazard. Mater 163 (2009) 213.
[22] K.K. Wong, C.K. Lee, K.S. Low, M.J. Haron, Chemosphere 50 (2003) 23.
[23] B.S. Creaven, M. Devereux, I. Georgieva, D. Karcz, M. McCann, N. Trendafilova, M. Walsh, Spectrochim. Acta Part A 84 (2011) 275.
[24] F.J. Guo, Coord. Chem. 62 (2009) 3606.
[25] I. Kani, Y.J. Aksu, Inorg. Organomet. Polym. 20 (2010) 69.
[26] Y.Y. Cheng, H.T. Chang, Y.C. Shiang, Y.L. Hung, C.K. Chiang, C.C. Huang, Anal. Chem. 81 (2009) 9433.
[27] K.W. Huang, C.J. Yu, W.L. Tseng, Biosens. Bioelectron. 25 (2010) 989.